frontiers in Marine Science

ORIGINAL RESEARCH
published: 26 February 2018
doi: 10.3389/fmars.2018.00059

Has Phytodetritus Processing by an Abyssal Soft-Sediment Community Recovered 26 Years after an Experimental Disturbance?

Tanja Stratmann[1*†], *Lisa Mevenkamp*[2†], *Andrew K. Sweetman*[3], *Ann Vanreusel*[2] *and Dick van Oevelen*[1]

[1] Department of Estuarine and Delta Systems, NIOZ Royal Netherlands Institute for Sea Research, Utrecht University, Yerseke, Netherlands, [2] Marine Biology Research Group, Ghent University, Ghent, Belgium, [3] The Lyell Centre for Earth and Marine Science and Technology, Heriot-Watt University, Edinburgh, United Kingdom

OPEN ACCESS

Edited by:
Ricardo Serrão Santos, University of the Azores, Portugal

Reviewed by:
Nikolaos Lampadariou, Hellenic Centre for Marine Research, Greece
George Andrew Wolff, University of Liverpool, United Kingdom

***Correspondence:**
Tanja Stratmann
tanja.stratmann@nioz.nl

[†]*These authors have contributed equally to this work.*

Specialty section:
This article was submitted to Deep-Sea Environments and Ecology, a section of the journal Frontiers in Marine Science

Received: *18 September 2017*
Accepted: *09 February 2018*
Published: *26 February 2018*

Citation:
Stratmann T, Mevenkamp L, Sweetman AK, Vanreusel A and van Oevelen D (2018) Has Phytodetritus Processing by an Abyssal Soft-Sediment Community Recovered 26 Years after an Experimental Disturbance? Front. Mar. Sci. 5:59. doi: 10.3389/fmars.2018.00059

The potential harvest of polymetallic nodules will heavily impact the abyssal, soft sediment ecosystem by removing sediment, hard substrate, and associated fauna inside mined areas. It is therefore important to know whether the ecosystem can recover from this disturbance and if so at which rate. The first objective of this study was to measure recovery of phytodetritus processing by the benthic food web from a sediment disturbance experiment in 1989. The second objective was to determine the role of holothurians in the uptake of fresh phytodetritus by the benthic food web. To meet both objectives, large benthic incubation chambers (CUBEs; 50 × 50 × 50 cm) were deployed inside plow tracks (with and without holothurian presence) and at a reference site (holothurian presence, only) at 4100 m water depth. Shortly after deployment, ^{13}C- and ^{15}N-labeled phytodetritus was injected in the incubation chambers and during the subsequent 3-day incubation period, water samples were taken five times to measure the production of ^{13}C-dissolved inorganic carbon over time. At the end of the incubation, holothurians and sediment samples were taken to determine biomass, densities and incorporation of ^{13}C and ^{15}N into bacteria, nematodes, macrofauna, and holothurians. For the first objective, the results showed that biomass of bacteria, nematodes and macrofauna did not differ between reference sites and plow track sites when holothurians were present. Additionally, meiofauna and macrofauna taxonomic composition was not significantly different between the sites. In contrast, total ^{13}C uptake by bacteria, nematodes and holothurians was significantly lower at plow track sites compared to reference sites, though the number of replicates was low. This result suggests that important ecosystem functions such as organic matter processing have not fully recovered from the disturbance that occurred 26 years prior to our study. For the second objective, the analysis indicated that holothurians incorporated 2.16 × 10^{-3} mmol labile phytodetritus C m^{-2} d^{-1} into their biomass, which is one order of

magnitude less as compared to bacteria, but 1.3 times higher than macrofauna and one order of magnitude higher than nematodes. Additionally, holothurians incorporated more phytodetritus carbon per unit biomass than macrofauna and meiofauna, suggesting a size-dependence in phytodetritus carbon uptake.

Keywords: stable isotopes, Pacific Ocean, DISCOL, C/N-ratio, stoichiometry, carbon limitation, Holothuroidea, deep-sea mining

INTRODUCTION

Abyssal plains, i.e., the ocean floor between 3,000 and 6,000 m water depth, cover more than 50% of the Earth's surface and form the largest ecosystem on earth (Smith et al., 2008). Although the remote abyssal plains seem to be far away from anthropogenic influences, they experience increased pressure from oil and gas extraction activities and disposal of litter and waste (Ramirez-Llodra et al., 2011). In the near future, they may also be affected by climate change (Sweetman et al., 2017), as well as by potential deep-sea mineral extraction of polymetallic nodules (Ramirez-Llodra et al., 2011; Petersen et al., 2016). Polymetallic nodules are potato-like deposits that grow extremely slowly at a rate of millimeters per million years (Guichard et al., 1978). They are typically found at the sediment surface at an average density of 15 kg m^{-2} in the Clarion-Clipperton Zone (CCZ, NE Pacific), 10 kg m^{-2} in the Peru Basin (SE Pacific) and 4.5 kg m^{-2} in the Central Indian Ocean Basin (Kuhn et al., 2017). Nodules provide hard substrate that is essential for some sessile epifauna and associated megafauna (Purser et al., 2016; Vanreusel et al., 2016).The extraction of polymetallic nodules will not only eliminate this hard substrate, but will also disturb and resuspend the surface sediment (Thiel and Tiefsee-Umweltschutz, 2001), which is critical for detritus feeding mobile epifauna and the biota that inhabit the sediment (Borowski and Thiel, 1998; Bluhm, 2001; Borowski, 2001).

We presently lack sufficient knowledge to assess if, and at what rate, the ecosystem will recover from these disturbances (Mengerink et al., 2014). The first insights on ecosystem recovery and resilience were provided by small-scale disturbance experiments that have been carried out at several sites in the Pacific and Indian Ocean (Jones et al., 2017). These studies focused on recovery of density and diversity of meiofauna, macrofauna, and megafauna (Ingole et al., 2000, 2005; Ahnert and Schriever, 2001; Bluhm, 2001; Borowski, 2001). For the DISCOL ("DISturbance and reCOLonization experiment;" Bluhm, 2001) area in the Peru Basin (tropical SE Pacific), in particular, it was found that recovery of megafauna densities after 26 years was between 11% (Anthozoa) and 167% (Holothuroidea) (Gollner et al., 2017). Macrofauna recovered to 85% within seven years (Borowski, 2001) and meiofauna densities after 26 years had recovered to 90% (Gollner et al., 2017). However, the recovery of key ecosystem functions such as nutrient cycling, organic matter processing, and secondary production (Thurber et al., 2014) has not been assessed in detail yet.

Pulse-chase experiments using stable isotopically labeled substrates have been used to study ecosystem functioning and food web dynamics in the deep sea (Middelburg, 2014). These studies are performed either *in-situ* with benthic landers (Moodley et al., 2002; Sweetman and Witte, 2008) or *ex-situ* with sediment cores onboard research vessels (Guilini et al., 2010). In both approaches, phytodetritus, e.g., diatoms or coccolithophores (Jeffreys et al., 2013), or zooplankton fecal pellets (Mayor et al., 2012) that have been enriched in ^{13}C and/ or ^{15}N are added to the benthic ecosystem (*pulse*) to track the uptake and processing of this material by microorganisms, meiofauna, metazoan macrofauna, and foraminifera (*chase*). Despite the high importance of deep-sea megafauna, dominated by holothurians, as e.g., grazers of labile phytodetritus (Miller et al., 2000; Gallucci et al., 2008; Amaro et al., 2010), logistic challenges of deep-sea research have so far hampered the inclusion of megafauna in these stable isotope studies. This represents a major gap in our understanding of abyssal food webs (van Oevelen et al., 2012). Due to slow recovery rates and high vulnerability of deep-sea megafauna to mechanical disturbance (Bluhm, 2001; Vanreusel et al., 2016; Stratmann et al., in review), insight on the contribution of megafauna to important ecosystem functions is particularly relevant in the context of deep-sea mining impact assessments.

In this study, we conducted pulse-chase experiments at the DISCOL experimental area (DEA) to quantify ecosystem recovery of an abyssal ecosystem following a sediment disturbance event that occurred 26 years prior to our study. The DEA is a 10.8 km^2 large circular area (Bluhm, 2001) that was plowed diametrically 78 times in 1989 (Foell et al., 1990, 1992) to induce a disturbance that would mimic small-scale mining of polymetallic nodules. We deployed newly designed benthic incubation chambers that enabled us to include larger megafauna in pulse-chase studies. A recent visit to the DEA allowed us to assess (1) the recovery of ecosystem functioning in the form of carbon uptake and partitioning 26 years after a disturbance event and (2) the contribution of holothurians to the total uptake of fresh phytodetritus.

MATERIALS AND METHODS

Design of the Benthic Incubation Chambers

Benthic incubation chambers (henceforth called CUBEs in reference to their cubical design) were designed by the Royal Netherlands Institute for Sea Research with a large Poly(methyl methacrylate) (PMMA) chamber (50 × 50 × 50 cm, **Figure 1A**, **Supplementary Figure 1**). The CUBEs have an open bottom to enclose a megafaunal specimen on the seafloor. Each CUBE is further equipped with a stirring plate to ensure homogenously mixed water and an injection port with a 30 mL syringe to add a tracer (e.g., phytodetritus or bromide) at a preset time.

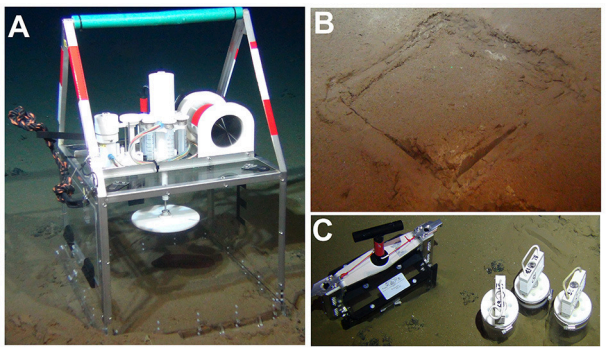

FIGURE 1 | *In-situ* pulse-chase tracer experiment with holothurian at 4,100 m depth in the Peru Basin. **(A)** Deployment of the benthic incubator (CUBE) over *Benthodytes* sp. in a plow track in the DEA west. **(B)** Imprint of CUBE in the sediment after its removal by ROV at the end of the incubation. **(C)** Sampling of sediment inside the CUBE imprint for macrofauna (bladecorer), meiofauna, bacteria, and sediment characteristics (pushcores). Photos by ROV Kiel 6000 (GEOMAR, Kiel, Germany).

A rosette with six 35 mL sampling syringes is fitted on the CUBE for repeated water sampling and a 6,000 m-rated oxygen optode (Contros HydroFlash® O_2; Kongsberg Maritime Contros GmbH, Germany) is inserted in the chamber top for continuous oxygen measurements. A titanium housing holds the battery pack, controller board and temperature sensor. The chamber has a PMMA door (22 × 42 cm) on one side that can be opened and closed by the ROV to allow sampling of enclosed specimens. We also noticed that a deployment with "the door open" significantly minimized sediment disturbance. Four ventilation valves in the top of the CUBE ensure that all air escapes during the descent, but that the CUBE remains sealed at the seafloor. All edges and corners are fortified with a stainless steel 316 frame that ends in a stainless-steel grip bar (total CUBE height: 100 cm). The stirring plate has a diameter of 20 cm, is adjustable in height and has an adjustable stirring capacity from 0 to 100% (0–18 rpm). Stirring tests using uranine as passive tracer for seven different stirring capacities (10, 20, 30, 40, 50, 75, 100%) showed that the uranine concentration reached an equilibrium in the CUBE between 1.5 min (100% stirring capacity) and 6.3 min (10% stirring capacity). This mixing speed is fast enough to consider the water column inside to be homogenously mixed during the incubation. The battery pack consists of 12 D-sized alkaline batteries connected in series (∼18 V power if new batteries are used) and supplies power to the motors of the sampling rosette, stirring plate, injection device and O_2 optode. The CUBEs run fully autonomously following a script that is saved on a micro SD or SDHC card and the program is activated when the ROV triggers a start flap, i.e., a flexible plastic flap at the side of the CUBE (**Figure 1A**).

Experimental Set-Up and Sampling Procedures

The study was conducted during RV Sonne cruise SO242-2 to the DEA (−88.45°E, −7.07°N; **Figure 2A**) in September 2015 and included three different treatments. Two CUBE incubations were performed at the southern reference station (**Figures 2A,C**) with an enclosed holothurian (one identified later as *Benthodytes* sp. and one as *Amperima* sp.) and are henceforth referred to as "Ref+hol." Three incubations were conducted inside the 6-m wide plow tracks (**Figures 2A,B**) each enclosing a holothurian (identified later as twice *Amperima* sp. and *Peniagone* sp. and will be referred to as "PT+hol") and two incubations inside the plow tracks without a holothurian, referred to as "PT-hol." We note that this (unbalanced) experimental design was a compromise following from practical and logistical limitations, while allowing us to focus on ecosystem recovery ("Ref+hol" vs. "PT+hol") and the impact of holothurians ("PT+hol" vs. "PT-hol").

The CUBEs were deployed on a dedicated lander (i.e., the elevator; Linke, 2010) that was placed at a specific location (reference site, disturbed site within a plow track) using a video-guided release system. The ROV KIEL 6000 lifted a CUBE from the elevator and placed it gently over a holothurian to trap it (**Figure 1A**, treatments "PT+hol" and "Ref+hol") or directly on the seafloor (treatment "PT-hol"). The incubation was subsequently started by moving the start flap. Each CUBE deployment lasted 3 days. The first water sample was taken after 45 min, followed by the injection of 0.5 g dry weight (DW) (equivalent to 40 mmol C m^{-2} and 5 mmol N m^{-2}) freeze-dried *Skeletonema costatum* (29 at% ^{13}C and 37 at% ^{15}N). Stirring capacity was increased from 50 to 100% for 10 min and then stopped for 45 min to allow for a homogeneous settling of the freeze-dried diatoms. Afterwards, stirring was set to 25% and subsequently water samples were taken at 0.07, 1, 2, and 3 days after the start of the incubation. Unfortunately, oxygen concentrations could not be measured due to the sensor malfunctioning. At the end of the experiment, the side door of the CUBE was opened and the holothurian was carefully sampled with the suction sampler into the suction container of the ROV. The CUBE was lifted and put aside to leave a clear imprint in the sediment (**Figure 1B**). A bladecorer (20.5 × 9 × 30 cm; designed by Max Planck Institute for Marine Microbiology, Germany) for macrofauna sampling was pressed into the sediment at a random place within the imprint square and released. The bladecorer was left in place until three push cores were taken from within the experimental area to minimize sediment disturbance (**Figure 1C**).

Aboard RV Sonne, the water samples were filtered through a 0.2 µm syringe filter in 20 mL headspace vials for DIC and ^{13}C-DIC concentration analysis and preserved by the addition of 20 µL 0.24 mol L^{-1} $HgCl_2$. The overlying water from the push cores was carefully siphoned off and sieved (32 µm). Subsequently, the cores were sliced in 0–2 and 2–5 cm intervals in a climate room at *in-situ* temperature (2.9°C) and meiofauna from the overlying water was added to the 0–2 cm layer. The different sediment layers of the three push cores from a single CUBE deployment were pooled and homogenized to reduce spatial variability and ensure sufficient amounts of sediment for the planned analyses. Subsequently, two 35 mL subsamples were taken and stored frozen at −21°C for bacterial specific phospholipid-derived fatty acid (PLFA) analysis, sediment porosity, bulk N/^{15}N and organic C/^{13}C

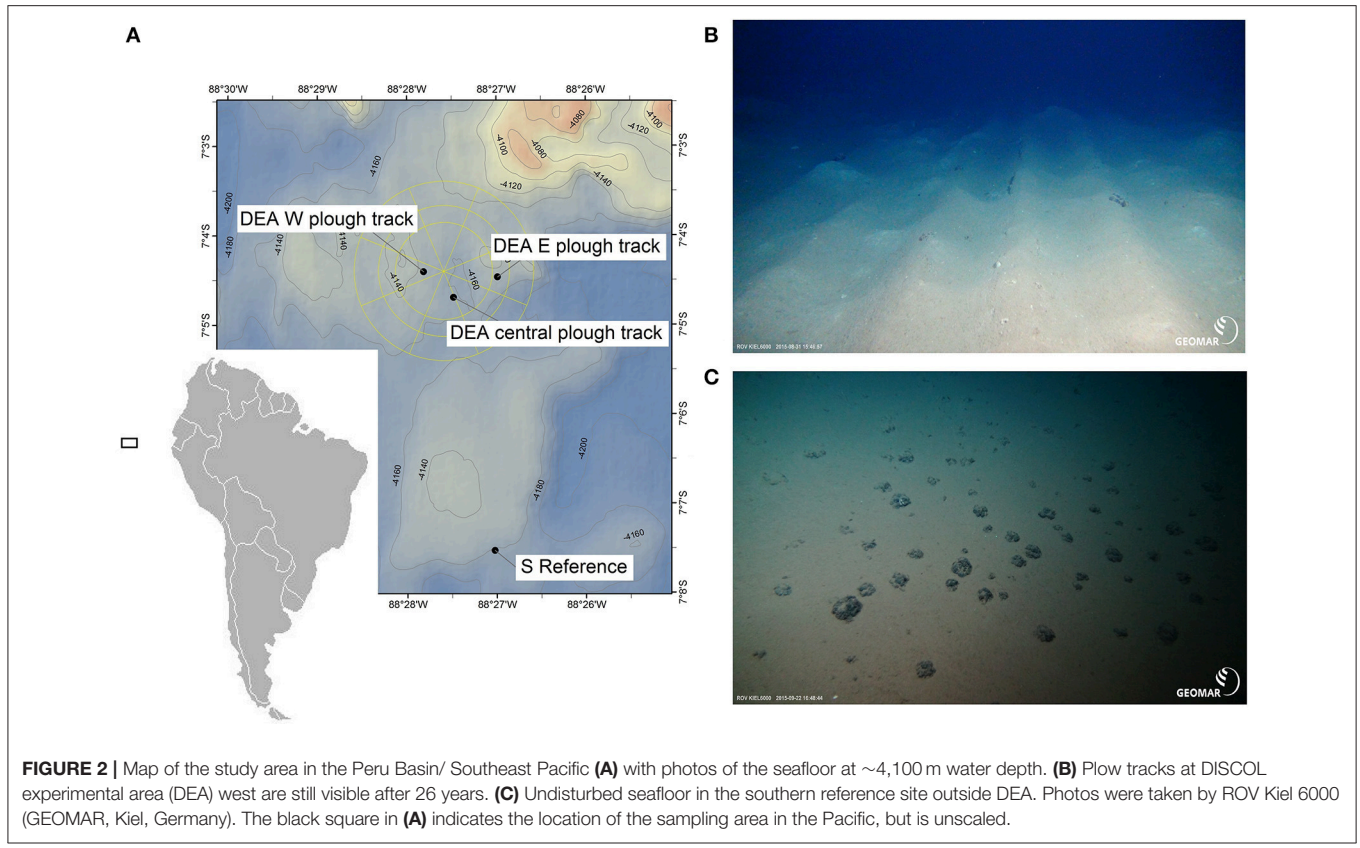

FIGURE 2 | Map of the study area in the Peru Basin/ Southeast Pacific **(A)** with photos of the seafloor at ∼4,100 m water depth. **(B)** Plow tracks at DISCOL experimental area (DEA) west are still visible after 26 years. **(C)** Undisturbed seafloor in the southern reference site outside DEA. Photos were taken by ROV Kiel 6000 (GEOMAR, Kiel, Germany). The black square in **(A)** indicates the location of the sampling area in the Pacific, but is unscaled.

determination. The remaining sediment was fixed in 4% borax-buffered formaldehyde for meiofauna analysis (abundance and isotope enrichment). The upper 5 cm of the sediment in the bladecorer was sieved over a 500 μm sieve with filtered seawater (0.7 μm) at *in-situ* temperature. All macrofauna were fixed in 4% borax-buffered formaldehyde.

Sediment Analysis

Sediment porosity was determined by the weight difference between wet sediment and freeze-dried sediment assuming a sediment density of 2.55 g cm^{-3} (Haeckel et al., 2001). The organic $C/^{13}C$ and $N/^{15}N$ of ∼20 mg freeze-dried, acidified sediment was measured with at Thermo Flash EA 1112 elemental analyzer (EA; Thermo Fisher Scientific, USA) coupled to a DELTA V Advantage Isotope Ratio Mass Spectrometer (IRMS; Thermo Fisher Scientific, USA).

Bacteria Analysis

Bacterial biomass and incorporation of phytodetritus ^{13}C into bacteria were determined through the analysis of bacterial-specific PLFAs. Lipids were extracted from ∼2.5 g freeze-dried, finely ground sediment with a modified Bligh and Dyer extraction method (Boschker et al., 1999; Moodley et al., 2002). The lipid extract was fractioned into different lipid classes on a silicic-acid column by sequentially eluting with chloroform (neutral lipids), acetone (glycolipids), and methanol (polar lipids). The polar lipid fraction was derivatized to fatty acid methyl esters (FAME) and measured on a HP 61530 gas chromatograph (Hewlet Packard/ Agilent, USA) coupled with a DELTA-Plus Isotope Ratio Mass Spectrometer (Thermo Fisher Scientific, USA) with a polar analytical column (ZB5-5MS; 60 m length, 0.32 mm diameter, 0.25 μm film thickness; Phenomenex, USA).

The bacterial biomass was calculated based on the concentration of the bacterial specific PLFAs i14:0, i15:0, a15:0, i16:0, and 18:1ω7c, assuming that these represent 28% of the C in all bacterial PLFA and that PLFAs represent 6% of the total C in bacterial cells (Middelburg et al., 2000).

Meiofauna Analysis

Meiofauna was extracted from sediment by washing the samples over a 32 μm sieve and subsequent density centrifugation of the fraction retained on the 32 μm sieve with Ludox HS40 (Dupont) at 3,000 rpm (specific density of 1.18; Heip et al., 1985). The centrifugation was repeated three times, the supernatant was sieved (32 μm) and fixed again in 4% borax-buffered formaldehyde. Meiofauna were organisms counted for density estimates and identified to higher taxon level with a stereomicroscope (50x magnification).

Due to the small body-size of meiofauna, several hundreds of organisms needed to be pooled to have sufficient biomass for the analysis of organic C, ^{13}C, N, and ^{15}N. Therefore only the most abundant taxon, i.e., nematodes, was analyzed. A total of 500 nematodes were randomly handpicked per sample (or less when

not enough nematodes were present in a sample) and transferred to a few drops of Milli-Q water in 8 × 5 mm silver capsules (pre-combusted for 4 h at 450°C). The samples were dried overnight at 60°C, acidified with 20 µL 2% HCl and dried again at 60°C on a hot plate. Capsules were closed and organic C and N content was analyzed following the procedure described above for sediment.

Macrofauna Analysis

Macrofauna was counted for density estimates and identified to lowest taxonomic level and when possible to family level in case of polychaetes using a stereomicroscope. For the analysis of organic C, ^{13}C, N, and ^{15}N, dried, whole organisms were packed in pre-combusted 8 × 5 mm silver capsules, measured following the procedure for meiofauna. Unfortunately, 39% of the macrofauna samples were compromised during sample preparation for the elemental analyzer after density determination and had to be discarded.

Megafauna Analysis

Individual holothurian specimen were retrieved from the ROV suction containers, measured for length, height and width and dissected to separate gut and gut contents from the other somatic tissue. All tissue samples were shock frozen in liquid nitrogen and stored at −21°C. After freeze-drying the somatic tissue excluding the gut tissue was manually ground to fine powder and organic C, ^{13}C, N, and ^{15}N were measured in ∼2 mg holothurian powder as described above for macrofauna.

For the holothurian biomass determination, wet weight (WW) of each specimen was calculated based on the length (L) of the organism using the length-wet weight relationship $WW = 0.859 \times L^{1.813}$ ($n = 13$, $R^2 = 0.68$) identified for intact holothurians from Brown et al. (in review). Holothurian WW was converted to DW using a conversion determined for the holothurians in the Peru Basin in Brown et al. (in review) ($DW = 0.04 \times WW + 0.13$; $n = 13$, $R^2 = 0.98$) and then converted into organic C using the organic C content measured for dried tissue sample of each individual (C content in holothurians ranged from 1.96 to 9.69%).

DIC Analysis

For the analysis of DIC and ^{13}C-DIC, He-gas was injected through the septum into the head-space vials to create a headspace of ∼1.5 mL. The sample was acidified with 10 µL concentrated H_3PO_4 per 1 mL water to transform all inorganic C into gaseous CO_2 in the headspace. From the headspace, a 500 µL sample was taken and injected into a Flash 1112 Series elemental analyzer (EA) coupled via a Conflo III to a Thermo Delta V continuous flow isotope ratio mass spectrometer (IRMS) for the analysis of DIC concentration and isotopic composition (Gillikin and Bouillon, 2007).

Calculations

The incorporation (I) of phytodetritus C and N into particulate organic carbon (POC) and particulate nitrogen (PN), i.e., phytodetritus C and N recovered from the sediment, and bacteria, meiofauna, several macrofauna specimen and megafauna was calculated as follows. The R_{sample} is the ratio of $^{13}C/^{12}C$ or $^{15}N/^{14}N$ in the samples and is calculated based on the $^{13}C/^{15}N$ output of the IRMS:

$$R_{sample} = (\delta^{13}C/1000 + 1) \times R_{standard} \text{ or}$$
$$R_{sample} = (\delta^{15}N/1000 + 1) \times R_{standard} \quad (1)$$

where $R_{standard}$ for C is 0.0111802 and for N it is 0.0036782. The fraction (F) of the heavy isotopes ^{13}C and ^{15}N in the sample (F_{sample}) and background ($F_{background}$) material is calculated as:

$$F = {}^{13}C/({}^{13}C + {}^{12}C) = R/(R+1) \quad (2)$$

The incorporation of phytodetrital C and N (I) is:

$$I = (F_{sample} - F_{background}) \times \textit{total C} \text{ or } \textit{N pool/phytodetritus enrichment} \quad (3)$$

Macrofauna incorporation rates could not be estimated for all incubations due to unfortunate sample loss (see above). Therefore, the total phytodetritus C and N incorporation rate is defined as the sum of bacteria and nematode phytodetritus C and N incorporation in the top (0–2 cm) and bottom sediment layer (2–5 cm) plus the phytodetritus C and N incorporation into holothurians.

The bulk carbon:nitrogen-ratio (C_{bulk}:N_{bulk}-ratio) of organisms (meiofauna and macrofauna) or somatic tissue (holothurians) and phytodetritus was calculated as the molar ratio. The C_{uptake}:N_{uptake}-ratio was calculated as incorporation of phytodetritus C in the organism divided by the incorporation of phytodetritus N in the organism.

The total biomass of nematodes was calculated as the biomass of an individual nematode (C content of individual nematode = C content of number of measured nematodes divided by number of measured nematodes) times the density of nematodes in the sediment that was determined during counting of meiofauna. The biomass of macrofauna was calculated as the taxon-specific (polychaetes, arthropods, nematodes) macrofauna density times the average tax on specific individual biomass.

Statistical Analysis

Due to the low number of replicates ($n = 2$ for Ref+hol, $n = 3$ for PT+hol, $n = 2$ for PT-hol), differences in density, biomass and ecosystem functioning, i.e., phytodetritus C and N uptake and phytodetritus C-DIC production, between treatments were assessed by comparing the 83.4% confidence intervals (CI). These 83.4% CI were calculated by bootstrapping 10,000 boots-trap replicates using the "boot" package in R (Canty and Ripley, 2017) and represent a type 1 error probability (α) of 0.05 (Knol et al., 2011). This means that the difference in means between treatments is statistically not significant for $\alpha = 0.05$ when the 83.4% CI overlap. Data are presented as mean with lower 83.4% CI—upper 83.4% CI, except for contributions to total density or uptake which are presented as mean ± standard deviation. The C_{uptake}:N_{uptake}-ratios and C_{uptake}:N_{uptake}-ratio were presented as median with 1st quantile and 3rd quantile.

For the analysis of differences in benthic community composition between treatments, the density data of meiofauna

and macrofauna of the upper 5 cm were combined and square-foot transformed before applying the "Analysis of Similarities" (ANOSIM) routine for Bray-Curtis similarity in PRIMER 6 (Clarke and Gorley, 2006).

A one-sample Wilcoxon signed-rank test on log_{10}-transformed data was conducted to determine whether the difference between the median C_{uptake}:N_{uptake}-ratio of nematodes, macrofauna or holothurians combined for all sites and the C_{uptake}:N_{uptake}-ratio of the added phytodetritus were significant.

RESULTS

Visual Inspection of the Sites

Plow marks from the 26-year old disturbance were clearly visible as several centimeter-high ripples and valleys (**Figure 2B**). The sediment surface inside the plow tracks was a mosaic of original brownish surface sediment and white patches originating from sediment that was turned upside down during plowing. The plowing effectively buried the polymetallic nodules into the sediment leaving the plow tracks cleared of the typical hard substrate-providing surface nodules. In contrast, the reference site (**Figure 2C**) had a very smooth brown sediment surface with a homogenous distribution of surface polymetallic nodules.

Benthic Biomass, Density, and Community Composition

Based on the 83.4% CIs, mean biomass of bacteria and macrofauna (**Table 1**) in the upper 5 cm of sediment did not differ between reference site, plow track site or presence of holothurians. In contrast, the mean nematode biomass in the lower (2–5 cm) sediment layer differed significantly between treatments PT-hol [0.22 (0.21–0.22) mmol C m^{-2}] and Ref+hol [0.19 (0.19–0.20) mmol C m^{-2}], but not between PT+hol and PT-hol or Ref+hol in the same sediment layer. Also, the mean nematode biomass in the upper sediment layer (0–2 cm) was not different between the reference sites, plow track site or presence of holothurians.

Total mean meiofauna density was not significantly different between the treatments based on the 83.4% CI (**Table 2**). Nematodes contributed most to the total meiofauna density in the upper 5 cm of sediment (Ref+hol: 88.43 ± 0.19%, PT+hol: 90.62 ± 1.36%, PT-hol: 88.33 ± 0.52%), followed by harpacticoid copepods (Ref+hol: 5.74 ± 0.70%, PT+hol: 5.01 ± 1.09%, PT-hol: 6.98 ± 0.11%) and nauplii (Ref+hol: 4.01 ± 0.77%, PT+hol: 2.92 ± 0.67%, PT-hol: 3.13 ± 0.58%).

Based on the 83.4% CI the total macrofauna densities of the different treatments were significantly different from each other (**Table 2**). About 25% of the macrofauna consisted of polychaetes at Ref+hol (26.14 ± 1.61%) and PT+hol (25.40 ± 9.91%). At PT-hol, polychaetes contributed only 8.33 ± 0.00% to the total macrofauna density and the macrofauna assemblage was dominated by harpacticoids (33.33 ± 0.00%), followed by isopods, tanaids, and nematodes that contributed each 12.50 ± 5.89% to the total macrofauna density. Large nematodes were the second largest contributor to macrofauna density in the Ref+hol treatment (21.59 ± 4.82%), whereas this role was taken by ostracods in the PT+hol treatment (15.08 ± 14.35%). When the combined meiofauna and macrofauna species composition in the upper 5 cm was compared, no significant difference was detected between the three treatments (ANOSIM: $p = 0.87$).

TABLE 1 | Mean biomass and (lower 84.3% CI – upper 84.3% CI) (mmol C m^{-2}) of bacteria, nematodes, and macrofauna in the three different treatments Ref+hol (incubation at reference station outside DEA including holothurians), PT+hol (incubation inside plow tracks inside DEA including holothurians), and PT-hol (incubation inside plow tracks inside DEA without holothurians).

		Bacteria biomass	Nematodes biomass	Macrofauna biomass
PT+hol	0–2 cm	13.81 (8.21–19.45)	0.27 (0.19–0.34)	
	2–5 cm	10.90 (2.47–19.20)	0.24 (0.15–0.33)	
	0–5 cm			0.94 (0.58–1.29)
PT-hol	0–2 cm	13.98 (11.44–16.52)	0.31 (0.15–0.46)	
	2–5 cm	17.82 (8.67–26.89)	0.22 (0.21–0.22)	
	0–5 cm			1.08 (0.37–1.79)
Ref+hol	0–2 cm	11.77 (11.73–11.81)	0.20 (0.16–0.24)	
	2–5 cm	12.73(9.32–16.12)	0.19 (0.19–0.20)	
	0–5 cm			1.90 (0.94–2.85)

TABLE 2 | Total mean density and (lower 84.3% CI—upper 84.3% CI) of meiofauna (ind. 10 cm^{-1}) and macrofauna (ind. m^{-2}) in the three different treatments Ref+hol (incubation at reference station outside DEA including holothurians), PT+hol (incubation inside plow tracks inside DEA including holothurians), and PT-hol (incubation inside plow tracks inside DEA without holothurians).

		Meiofauna density	Macrofauna density
PT+hol	0–2 cm	122 (108–136)	
	2–5 cm	81 (52–111)	
	0–5 cm		363 (343–383)
PT-hol	0–2 cm	118 (82–155)	
	2–5 cm	52 (43–61)	
	0–5 cm		654 (654–654)
Ref+hol	0–2 cm	108 (101–114)	
	2–5 cm	62 (56–69)	
	0–5 cm		518 (439–599)

Phytodetritus Processing

The total mean amount of phytodetritus C (mmol C m^{-2}) that was incorporated into bacteria, nematodes and holothurians (if present) was 0.39 (0.56–1.42) in the PT-hol treatment, 0.99 (0.57–1.43) in the PT+hol treatment and 2.36 (1.80–2.91) in the Ref+hol treatment (**Figures 3A–C**). Based on the 83.4% CI, phytodetritus C uptake by bacteria (mmol C m^{-2}) in the upper sediment layer was significantly different between Ref+hol (0.271–0.447) and PT-hol (0.131–0.269). In the lower sediment layer phytodetritus C uptake by bacteria (mmol C m^{-2}) differed significantly between Ref+hol (0.461–0.509) and PT+hol (0.013–0.040) and between Ref+hol (0.271–0.447) and PT-hol (0.035–0.338). Nematodes in the 0–2 cm

sediment layer from the PT-hol treatment (1.10×10^{-3} – 1.90×10^{-3} mmol C m^{-2}) incorporated significantly more phytodetritus C than nematodes from the same sediment layer of the Ref+hol treatment (6.00×10^{-4} – 9.00×10^{-4} mmol C m^{-2}). In the 2–5 cm sediment layer, the uptake of phytodetritus C (mmol C m^{-2}) by nematodes was in the same range at Ref+hol [4.50×10^{-4} (3.00×10^{-4} – 6.00×10^{-4})] and PT+hol [4.33×10^{-4} (3.00×10^{-4} – 6.00×10^{-4})], but less than at PT-hol [8.50×10^{-4} (6.00×10^{-4} – 1.10×10^{-3})]. Holothurians incorporated (not significantly) more phytodetritus C in treatment Ref+hol [1.52 (1.03–2.00) mmol C m^{-2}] than in treatment PT+hol [0.71 (0.29–1.11) mmol C m^{-2}], but had also a smaller biomass (mmol C ind^{-1}) in the later [Ref+hol: 122.04 (114.60–129.40); PT+hol: 36.77 (28.60–44.85)]. Most of the phytodetritus C (mmol C m^{-2}) that was added to the CUBEs was recovered in the sediment (POC) [Ref+hol: 5.02 (5.01–5.03), PT+hol: 7.29 (2.76–11.80), PT-hol: 6.47 (4.91–8.01); **Figure 3D**] and in the gut content of holothurians [Ref+hol: 0.84 (0.02–1.64), PT+hol: 0.43 (0.03–0.82)]. Respiration of phytodetritus C-DIC (mmol C m^{-2}) occurred linearly over time (**Figure 4**) and after 3 days of incubation it was 3.19 (2.97–3.42) at PT-hol, 2.22 (1.59–2.86) at PT+hol and 3.07 (2.65–3.49) at Ref+hol (**Figure 3E**). Hence, based on the 83.4% CI, phytodetritus C-DIC respiration was significantly lower in treatment PT+hol compared to treatment PT-hol.

Nematodes incorporated between 8.52×10^{-7} (5.83×10^{-7} – 1.12×10^{-6}) mmol N m^{-2} phytodetritus N (PT+hol) and 1.51×10^{-6} (1.23×10^{-6} – 1.78×10^{-6}) mmol N m^{-2} phytodetritus N (PT-hol; **Figure 5**) and therefore significantly less phytodetritus N at PT+hol than at PT-hol. Holothurians took up 0.15 (0.04 – 0.26) mmol N m^{-2} phytodetritus N in treatment PT+hol and 0.31 (0.20–0.41) mmol N m^{-2} phytodetritus N in treatment Ref+hol (**Figure 5**). Between 0.88 (0.36–1.40) mmol N m^{-2} phytodetritus N (PT+hol) and 1.06 (0.73–1.38) mmol N m^{-2} phytodetritus N (Ref+hol) was traced back in the sediment (PN; **Figure 5**).

C:N-Ratio

The phytodetritus that was added in the pulse-chase experiment had a C_{uptake}:N_{uptake}-ratio of 6.54 and C_{bulk}:N_{bulk}-ratio of 7.73. The (median) C_{uptake}:N_{uptake}-ratio of nematodes from both sediment layers combined ($n = 7$), macrofauna ($n = 20$) and holothurians ($n = 5$) was 16.56 (1st quantile: 14.34, 3rd quantile: 7.75), 11.44 (1st quantile: 9.38, 3rd quantile: 18.74), and 4.88 (1st quantile: 4.88, 3rd quantile: 5.06), respectively (**Figure 6**). The C_{bulk}:N_{bulk}-ratios were 7.12 (1st quantile: 6.57, 3rd quantile: 7.68), 5.57 (1st quantile: 3.62, 3rd quantile: 6.27), and 4.48 (1st quantile: 4.46, 3rd quantile: 4.63) for nematodes, macrofauna and holothurians, respectively. The difference between the median of the $\log_{10}$-transformed C_{uptake}:N_{uptake}-ratios of nematodes, macrofauna, somatic tissue of holothurians and the $\log_{10}$-transformed C_{uptake}:N_{uptake}-ratio of the added phytodetritus (0.82) was significant for nematodes ($Z = 2.48$, $p = 0.01$) and macrofauna ($Z = 3.92$, $p \leq 0.001$), but not for holothurians ($Z = -0.67$, $p = 0.63$).

DISCUSSION

This study shows that the ecosystem function of a previously disturbed seafloor had not completely recovered 26 years post-disturbance. Here we relate these results to other studies on small-scale deep-sea disturbances. We also compare the processing of labile phytodetritus by the benthos with similar pulse-chase studies and discuss the role of holothurians in deep-sea ecosystem functioning.

Recovery of Ecosystem Functioning from Deep-Sea Mining

As ecosystem functions in the deep sea are often interrelated to ecosystem services, such as nutrient regeneration and fisheries (Thurber et al., 2014), it is of major concern to decipher which processes of ecosystem functioning are able to recover from deep-sea mining and over what timescales. However, only few studies on ecosystem functions in deep-sea disturbance experiments have been conducted so far, hence a direct comparison between studies is cumbersome.

Our study showed that the bacteria in the 2–5 cm sediment layer did not incorporate phytodetritus C in equal amounts at reference sites compared to plow track sites. This is intriguing, because bacteria can incorporate up to 32% of the total processed label at the Pakistan margin (Woulds et al., 2009) and contribute 74% to total sediment community oxygen consumption at the lower continental slope and in abyssal plains (Heip et al., 2001). Reasons for this difference could be a varying level of sediment reworking by the holothurians inside the CUBEs that made more or less phytodetritus accessible to the subsurface bacteria or a different bacteria composition in the 2–5 cm sediment layer. During the plowing of the seafloor in 1989 parts of the surface sediment were removed and sediment was relocated inside the plow tracks. Hence, the sediment of the 2–5 cm layer in the reference area may be different from the 2–5 cm layer inside the plow tracks. This sediment difference may also cause a concurrent difference in the bacterial composition.

When comparing the total amount of phytodetritus C incorporated in bacteria and nematodes in the upper 5 cm of sediment and taken up by holothurians, the uptake was significantly lower at plow track sites compared to reference sites. This difference might be caused by lower, though not significantly, uptake of phytodetritus carbon by holothurians at the plow track site compared to the reference site. However, it might also indicate that ecosystem function in the form of phytodetritus C processing takes more than 26 years in the DEA to recover from the small-scale disturbance experiment in 1989. In contrast, ecosystem function in the form of respiration of large megafauna, i.e., holothurians, in the DISCOL area recovers faster. Stratmann et al. (in review) compared the respiration rates of holothurians in plow tracks inside DEA ("disturbed") with the respiration rates of holothurians outside plow tracks inside DEA ("undisturbed") and with rates from holothurians at reference sites ("reference") ∼4 km away from DEA. Measured rates of oxygen consumption were not significantly different at the disturbed, undisturbed and reference sites,

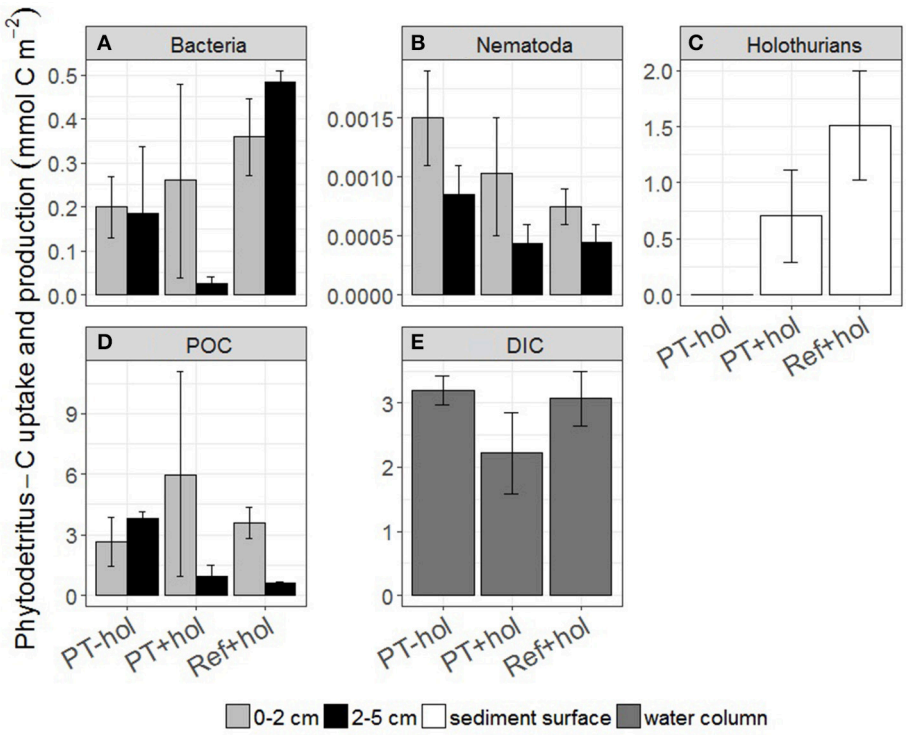

FIGURE 3 | Uptake and production of phytodetritus carbon (in mmol C m^{-2}) **(A)** bacteria, **(B)** Nematoda, **(C)** holothurians, **(D)** POC, i.e., phytodetritus C recovered from the sediment, and **(E)** DIC per sediment depth interval (in cm) and treatment. Error bars show the 83.4% confidence intervals. PT-hol, incubation inside plow tracks inside DEA without holothurian; PT+hol, incubation inside plow tracks inside DEA including holothurians; Ref+hol, incubation at the reference station outside DEA including holothurians.

indicating holothurian community respiration recovery within 26 years.

While future deep-sea mining is unlikely in the Peru Basin, exploration licenses have been issued in the CCZ. Here, ecosystem functioning in the form of nutrient cycling and sediment community oxygen consumption was reported for the French claim of the CCZ (Khripounoff et al., 2006). The authors deployed a benthic lander at a reference station and inside a 2.5 m-wide mining track, which was created in 1978 by dredging away the upper 4.5 cm of the sediment during a small-scale deep-sea mining experiment (Khripounoff et al., 2006). Sediment community oxygen consumption and nutrient fluxes of silicate, nitrate and phosphate were not different between the reference and disturbed location 26 years after the disturbance (Khripounoff et al., 2006), leading the authors to conclude that ecosystem functioning in terms of nutrient cycling had recovered.

Although these studies indicate that ecosystem function recovery takes at least 26 years, time scales for recovery from industrial-size deep-sea mining scenarios will likely be much larger. The DISCOL experiment was conducted in a relatively lightly disturbed area of 10.8 km^2, of which only about 22% were plowed within a month (Thiel and Schriever, 1989). In contrast, a single mining operation will likely remove polymetallic nodules over an area of 300–800 km^2 per year (Smith et al., 2008) and last for 15–30 years (Levin et al., 2016). Moreover, we did not take cumulative effects of deep-sea mining into account like the overlap of sediment plumes from close-by mining operations, changes in POC export fluxes due to climate-change or biodiversity loss due to deep-sea mining (Levin et al., 2016; Sweetman et al., 2017; Van Dover et al., 2017; Yool et al., 2017).

Role of Holothurians in Labile Phytodetritus Uptake

Another main objective of our study was to quantify the role of holothurians in phytodetritus processing. Due to an unfortunate loss of macrofauna samples, we have insufficient data to determine the total phytodetritus uptake by macrofauna except for one deployment. In this deployment (PT+hol), the macrofauna incorporated a total of 1.66×10^{-3} mmol phytodetritus C m^{-2} d^{-1} (0.4% of total uptake), suggesting that macrofauna play a comparatively limited role in the phytodetritus uptake in the Peru Basin. This is also supported by a comparison with *in-situ* studies on short-term phytodetritus processing by Woulds et al. (2009). At sites between 1,200 and 1,850 m at the Pakistan margin metazoan macrofauna took up between (mean ± std) 1 ± 0.5 and 4 ± 1% of the processed label (Woulds et al., 2009). Therefore, the role of holothurians in the processing of phytodetritus at the DISCOL

site can be estimated by neglecting the missing macrofauna contribution. However, this will overestimate the importance of holothurians, because the megafauna density in the CUBEs (1 holothurian specimen 0.25 m^{-2}, extrapolated to 4 holothurian specimen 1 m^{-2}) is two orders of magnitudes higher than under natural conditions (0.02 holothurian specimen m^{-2}; Stratmann et al., in review). To correct for the scale-effect of the incubation chamber and allow translation of the results to natural conditions, we multiplied the average holothurian uptake (0.09 mmol phytodetritus C $ind.^{-1}$ d^{-1}) with the holothurian density in the Peru Basin (240 ind. ha^{-1}; Stratmann et al., in review) to find a daily uptake of phytodetritus C by holothurians of 2.16×10^{-3} mmol phytodetritus C m^{-2} d^{-1}. Hence, based on data from the PT+hol treatment, the contribution of holothurian incorporation of labile phytodetritus to the total uptake of this carbon pool in the Peru Basin is one order of magnitude lower than the contribution of bacteria (7.30×10^{-2} mmol phytodetritus C m^{-2} d^{-1}), but one order of magnitude higher than the contribution of nematodes (4.80×10^{-4} mmol phytodetritus C m^{-2} d^{-1}). It is also 1.3 times larger than the contribution of macrofauna (1.66×10^{-3} mmol phytodetritus C m^{-2} d^{-1}) assuming that the uptake measured for this specific incubation is representative for the whole experiment. Even though bacterial uptake is one order of magnitude higher than the megafauna uptake, the uptake of megafauna is the highest of the metazoans suggesting that their activity should be considered in the structure of deep benthic food webs.

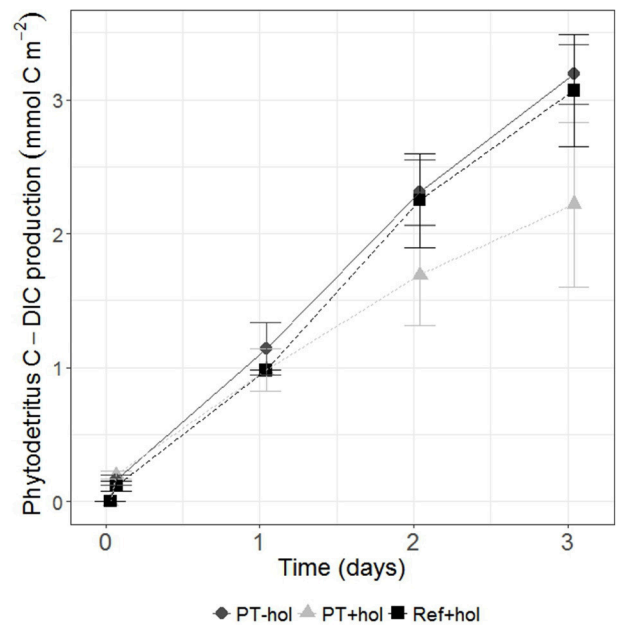

FIGURE 4 | Production of phytodetritus C-DIC (in mmol C m^{-2}) over time (in days) for all treatments. Error bars show the 83.4% confidence intervals. PT-hol, incubation inside plow tracks inside DEA without holothurians; PT+hol, incubation inside plow tracks inside DEA including holothurians; Ref+hol, incubation at the reference station outside DEA including holothurians.

Size-Class Dependent Uptake of Phytodetritus

Because half of the labile detritus that reached the seafloor on the Porcupine Abyssal Plain (PAP) in the NE Atlantic was modeled to be available for deposit feeders (Durden et al., 2017), it is interesting to investigate which size class of metazoan deposit-feeding benthos will most likely benefit from it. Levin et al.

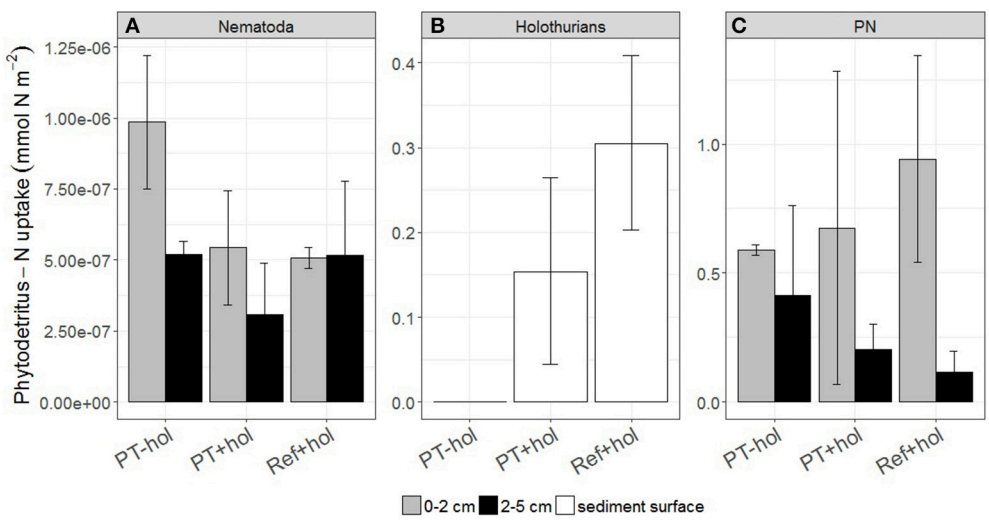

FIGURE 5 | Uptake of phytodetritus nitrogen (in mmol N m^{-2}) by **(A)** Nematoda, **(B)** holothurians, and **(C)** particulate nitrogen (PN), i.e., phytodetritus N recovered from the sediment, per sediment depth interval (in cm) and treatment. Error bars show the 83.4% confidence intervals. PT-hol, incubation inside plow tracks inside DEA without holothurians; PT+hol, incubation inside plow tracks inside DEA including holothurians; Ref+hol, incubation at the reference station outside DEA including holothurians.

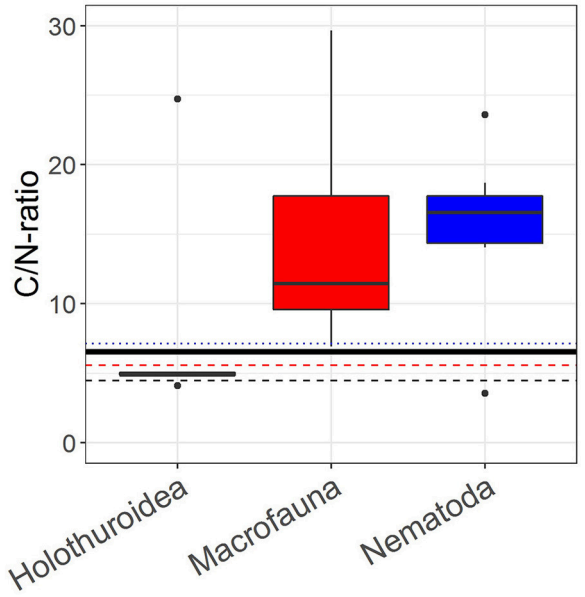

FIGURE 6 | Boxplots of the C_{uptake}:N_{uptake}-ratio, i.e., the incorporation of phytodetritus C in the organism divided by the incorporation of phytodetritus N in the organism, of holothurians ($n = 5$), macrofauna ($n = 20$), and nematodes ($n = 14$). The black solid line represents the C:N-ratio of the added phytodetritus (*Skeletonema costatum*), the black dashed line shows the median C:N-ratio, i.e. the molecular C:N-ratio, of somatic tissue of holothurians, the red dashed line shows the median C:N-ratio of macrofauna and the blue dotted line the median C:N-ratio of nematodes.

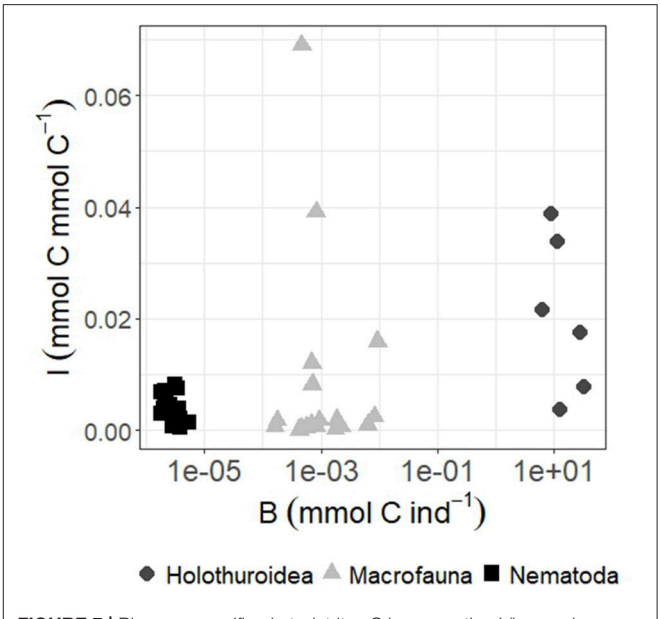

FIGURE 7 | Biomass-specific phytodetritus C incorporation I (in mmol phytodetritus C mmol C−1) per individual biomass B (mmol C ind−1) of holothurians, macrofauna, and Nematoda.

(1999) hypothesized that larger macrofauna organisms have better access to freshly deposited organic matter than smaller macrofauna organisms and therefore would be first in taking it up. These authors tested this hypothesis in one of the first *in-situ* tracer studies at the North Carolina slope (NE Atlantic). The regression of dry weight of macrofauna against diatom tracer uptake across taxa showed no relation with macrofaunal body size (Levin et al., 1999). However, the tested size was limited to macrofauna (>300 μm), whereas in the present study, we studied a substantially broader size spectrum ranging from nematodes/meiofauna (32 μm to 1 mm; 10^{-6} to 10^{-5} mmol C ind^{-1}), macrofauna (>500 μm, 10^{-4} to 10^{-2} mmol C ind^{-1}) to holothurians (>1 cm; 10^{0} to 10^{2} mmol C ind^{-1}) (**Figure 7**). A non-linear regression analysis of these data shows a highly significant positive relationship between individual size B and biomass-specific phytodetritus carbon uptake I [$I = 0.09B^{0.4}$; $n = 43$, $R^2 = 0.78$; $F_{(1,42)} = 145.9$, $p \leq 0.0001$]. Hence, our results suggest that larger organisms in the deep-sea may be more important in exploiting labile phytodetritus than smaller ones and therefore the link between surface productivity and organism productivity might be stronger for larger fauna as opposed to smaller size classes. However, the holothurians we included are selective feeding species, i.e., *Peniagone* sp. and *Amperima* sp. (Wigham et al., 2003; FitzGeorge-Balfour et al., 2010). It will be interesting to find out how strong the correlation between size class and fresh phytodetritus uptake is when other feeding types, such as the fermenters *Psychropotes longicauda* and *Pseudostichopus villosus* (Roberts et al., 2001), conveyor belt feeders or funnel feeders (Massin, 1982), are included.

C:N Stoichiometry

The results of the faunal uptake data were also explored for a potential size-dependent difference in uptake of phytodetritus carbon compared to nitrogen. A comparison of C_{uptake}:N_{uptake}-ratio showed that nematodes and macrofauna took up more phytodetritus carbon relative to phytodetritus nitrogen, whereas holothurians incorporated slightly more phytodetritus nitrogen relative to phytodetritus carbon when comparing it to the food source *S. costatum* (**Figure 6**). The C_{uptake}:N_{uptake}-ratio of the incorporated phytodetritus by nematodes and macrofauna was also higher than the bulk chemical composition of their body tissue, suggesting that they retained preferentially more carbon as compared to nitrogen. Such a dissimilar incorporation has been used to infer carbon vs. nitrogen limitation of benthic organisms. For example, a higher assimilation efficiency or proteinaceous N (mean ± std: 24.6 ± 10.5%) was found for the shallow-water mussel *Mytilus edulis* as compared to carbohydrates (16.7 ± 7.1%) or proteinaceous C (9.5 ± 3.1%) (Kreeger et al., 1996). This led the authors to conclude that *M. edulis* was more nitrogen limited than energy or protein limited and the higher assimilation efficiency of nitrogen would be a strategy to compensate for the low nitrogen content in their food. Although based on a comparatively short incubation time, the higher carbon retention as compared to nitrogen by nematodes and macrofauna may indicate that the nematodes and macrofauna at this specific site are more carbon or energy limited as opposed to nitrogen limited.

CONCLUSION

This is one of the few studies that investigate ecosystem function in an abyssal plain that was previously disturbed by a mimicked deep-sea mining experiment. Despite the low number of replications, the results indicate that the processing of fresh phytodetritus has not fully recovered after 26 years as the uptake of fresh phytodetritus by bacteria, nematodes and holothurians is significantly lower in plow tracks compared to reference sites.

Furthermore, the deployment of large (0.25 m^2) benthic incubation chambers allowed to determine the role of holothurians in the uptake of phytodetritus and showed that their uptake is highest compared to the other metazoans (meiofauna, macrofauna). The analysis of size-class dependent uptake of the phytodetritus resulted in a higher biomass-specific uptake of phytodetritus for holothurians than for nematodes implying that for the metabolism of holothurians phytodetritus is relatively more important than for the metabolism of smaller size classes. Additionally, the elevated C:N-ratios of incorporated phytodetritus in nematodes and macrofauna relative to their tissue C:N ratio let us speculate that these benthic organisms are likely more carbon than nitrogen limited at this particular study site.

AUTHORS CONTRIBUTIONS

AS, DvO, and AV: generated the project funding and conceived the idea of this experiment; AS, DvO, TS, and LM: performed the experiment, collected and analyzed the data; TS, LM, and DvO interpreted the data; TS and DvO: wrote the manuscript with input from all authors.

ACKNOWLEDGMENTS

We thank the captain and crew of RV Sonne as well as the ROV Kiel 6000 team from Geomar, Kiel for their excellent support during cruise SO242-2. We are grateful for the technical assistance by Pieter van Rijswijk and Peter van Breugel (NIOZ) and we thank Ina Stratmann (University of Paderborn) for preparing the technical drawing of the CUBE. Yann Marcon (Marum) is thanked for preparing the map of the study site. This research has received funding from the European Union Seventh Framework Programme (FP7/2007-2013) under the MIDAS project, grant agreement n° 603418, the JPI Oceans—Ecological Aspects of Deep Sea Mining project (NWO-ALW grant 856.14.002) and the Bundesministerium für Bildung und Forschung (BMBF) grant n° 03F0707A-G.

SUPPLEMENTARY MATERIAL

The Supplementary Material for this article can be found online at: https://www.frontiersin.org/articles/10.3389/fmars.2018.00059/full#supplementary-material

Supplementary Figure 1 | Technical drawing of the benthic incubation chamber CUBE with indicated dimensions given in mm. 1, oxygen optode; 2, injection device with the start flap; 3, stirring plate; 4, sampling rosette six 35 mL sampling syringes. The arrow points toward the start flap.

Data Availability

The raw data to this article can be found at: https://doi.pangaea.de/10.1594/PANGAEA.885565

REFERENCES

Ahnert, A., and Schriever, G. (2001). Response of abyssal Copepoda Harpacticoida (Crustacea) and other meiobenthos to an artificial disturbance and its bearing on future mining for polymetallic nodules. *Deep Sea Res. II* 48, 3779–3794. doi: 10.1016/S0967-0645(01)00067-4

Amaro, T., Bianchelli, S., Billett, D., Cunha, M., Pusceddu, A., and Danovaro, R. (2010). The trophic biology of the holothurian Molpadia musculus: implications for organic matter cycling and ecosystem functioning in a deep submarine canyon. *Biogeosciences* 7, 2419–2432. doi: 10.5194/bg-7-2419-2010

Bluhm, H. (2001). Re-establishment of an abyssal megabenthic community after experimental physical disturbance of the seafloor. *Deep Sea Res. II* 48, 3841–3868. doi: 10.1016/S0967-0645(01)00070-4

Borowski, C. (2001). Physically disturbed deep-sea macrofauna in the Peru Basin, southeast Pacific, revisited 7 years after the experimental impact. *Deep Sea Res. II* 48, 3809–3839. doi: 10.1016/S0967-0645(01)00069-8

Borowski, C., and Thiel, H. (1998). Deep-sea macrofaunal impacts of a large-scale physical disturbance experiment in the Southeast Pacific. *Deep Sea Res. II* 45, 55–81. doi: 10.1016/S0967-0645(97)00073-8

Boschker, H., De Brouwer, J., and Cappenberg, T. (1999). The contribution of macrophyte-derived organic matter to microbial biomass in salt-marsh sediments: stable carbon isotope analysis of microbial biomarkers. *Limnol. Oceanogr.* 44, 309–319. doi: 10.4319/lo.1999.44.2.0309

Canty, A., and Ripley, B. (2017). *boot: Bootstrap R (S-Plus) Functions.* R package version 1.3-19.

Clarke, K. R., and Gorley, R. N. (2006). *PRIMER v6: Manual/Tutorial*. Plymouth: PRIMER-E.

Durden, J. M., Ruhl, H. A., Pebody, C., Blackbird, S. J., and van Oevelen, D. (2017). Differences in the carbon flows in the benthic food webs of abyssal hill and plain habitats. *Limnol. Oceanogr.* 62, 1771–1782. doi: 10.1002/lno.10532

FitzGeorge-Balfour, T., Billett, D. S., Wolff, G. A., Thompson, A., and Tyler, P. A. (2010). Phytopigments as biomarkers of selectivity in abyssal holothurians; interspecific differences in response to a changing food supply. *Deep Sea Res. II* 57, 1418–1428. doi: 10.1016/j.dsr2.2010.01.013

Foell, E., Thiel, H., and Schriever, G. (1990). "DISCOL: a long-term, large-scale, disturbance-recolonization experiment in the abyssal eastern tropical South Pacific Ocean," in *Offshore Technology Conference* (Houston).

Foell, E., Thiel, H., and Schriever, G. (1992). DISCOL: a long-term, large-scale, disturbance-recolonization experiment in the abyssal eastern tropical South Pacific Ocean. *Min. Eng. Littleton* 44, 90–94.

Gallucci, F., Sauter, E., Sachs, O., Klages, M., and Soltwedel, T. (2008). Caging experiment in the deep sea: efficiency and artefacts from a case study at the Arctic long-term observatory HAUSGARTEN. *J. Exp. Mar. Biol. Ecol.* 354, 39–55. doi: 10.1016/j.jembe.2007.10.006

Gillikin, D. P., and Bouillon, S. (2007). Determination of $\delta^{18}O$ of water and $\delta^{13}C$ of dissolved inorganic carbon using a simple modification of an elemental analyser-isotope ratio mass spectrometer: an evaluation.

Rapid Commun. Mass Spectrom. 21, 1475–1478. doi: 10.1002/rcm.2968

Gollner, S., Kaiser, S., Menzel, L., Jones, D. O., Brown, A., Mestre, N. C., et al. (2017). Resilience of benthic deep-sea fauna to mining activities. *Mar. Environ. Res.* 129, 76–101. doi: 10.1016/j.marenvres.2017.04.010

Guichard, F., Reyss, J. L., and Yokoyama, Y. (1978). Growth rate of manganese nodule measured with 10Be and 26Al. *Nature* 272, 155–156. doi: 10.1038/272155a0

Guilini, K., Oevelen, D. V., Soetaert, K., Middelburg, J. J., and Vanreusela, A. (2010). Nutritional importance of benthic bacteria for deep-sea nematodes from the Arctic ice margin: results of an isotope tracer experiment. *Limnol. Oceanogr.* 55, 1977–1989. doi: 10.4319/lo.2010.55.5.1977

Haeckel, M., König, I., Riech, V., and Weber, M. E. (2001). Pore water profiles and numerical modelling of biogeochemical processes in Peru Basin deep-sea sediments. *Deep Sea Res. II* 48, 3713–3736. doi: 10.1016/S0967-0645(01)00064-9

Heip, C., Duineveld, G., Flach, E., Graf, G., Helder, W., Herman, P., et al. (2001). The role of the benthic biota in sedimentary metabolism and sediment-water exchange processes in the Goban Spur area (NE Atlantic). *Deep Sea Res. II* 48, 3223–3243. doi: 10.1016/S0967-0645(01)00038-8

Heip, C., Vincx, M., and Vranken, G. (1985). The ecology of marine nematodes. *Oceanogr. Mar. Biol.* 23, 399–489.

Ingole, B., Ansari, Z., Rathod, V., and Rodrigues, N. (2000). Response of meiofauna to immediate benthic disturbance in the Central Indian Ocean Basin. *Mar. Georesour. Geotec.* 18, 263–272. doi: 10.1080/10641190009353794

Ingole, B., Pavithran, S., and Ansari, Z. A. (2005). Restoration of deep-sea macrofauna after simulated benthic disturbance in the Central Indian Basin. *Mar. Georesour. Geotec.* 23, 267–288. doi: 10.1080/10641190500446573

Jeffreys, R. M., Burke, C., Jamieson, A. J., Narayanaswamy, B. E., Ruhl, H. A., Smith Jr, K. L., et al. (2013). Feeding preferences of abyssal macrofauna inferred from *in situ* pulse chase experiments. *PLoS ONE* 8:e80510. doi: 10.1371/journal.pone.0080510

Jones, D. O., Kaiser, S., Sweetman, A. K., Smith, C. R., Menot, L., Vink, A., et al. (2017). Biological responses to disturbance from simulated deep-sea polymetallic nodule mining. *PLoS ONE* 12:e0171750. doi: 10.1371/journal.pone.0171750

Khripounoff, A., Caprais, J.-C., Crassous, P., and Etoubleau, J. (2006). Geochemical and biological recovery of the disturbed seafloor in polymetallic nodule fields of the Clipperton-Clarion Fracture Zone (CCFZ) at 5,000-m depth. *Limnol. Oceanogr.* 51, 2033–2041. doi: 10.4319/lo.2006.51.5.2033

Knol, M. J., Pestman, W. R., and Grobbee, D. E. (2011). The (mis) use of overlap of confidence intervals to assess effect modification. *Eur. J. Epidemiol.* 26, 253–254. doi: 10.1007/s10654-011-9563-8

Kreeger, D., Hawkins, A., and Bayne, B. (1996). Use of dual-labeled microcapsules to discern the physiological fates of assimilated carbohydrate, protein carbon, and protein nitrogen in suspension-feeding organisms. *Limnol. Oceanogr.* 41, 208–215. doi: 10.4319/lo.1996.41.2.0208

Kuhn, T., Wegorzewski, A., Rühlemann, C., and Vink, A. (2017). "Composition, formation, and occurrence of polymetallic nodules," in *Deep-Sea Mining*, ed R. Sharma (Cham: Springer), 23–63.

Levin, L. A., Mengerink, K., Gjerde, K. M., Rowden, A. A., Van Dover, C. L., Clark, M. R., et al. (2016). Defining "serious harm" to the marine environment in the context of deep-seabed mining. *Mar. Policy* 74, 245–259. doi: 10.1016/j.marpol.2016.09.032

Levin, L., Blair, N., Martin, C., DeMaster, D., Plaia, G., and Thomas, C. (1999). Macrofaunal processing of phytodetritus at two sites on the Carolina margin: *in situ* experiments using 13C-labeled diatoms. *Mar. Ecol. Prog. Ser.* 182, 37–54. doi: 10.3354/meps182037

Linke, P. (2010). "Cruise Report SO-210 ChiFlux - Identification and investigation of fluid flux, mass wasting and sediments in the forearc of the central Chilean subduction zone - Valparaiso - Valparaiso 23.09. – 01.11.2010," in *Berichte aus dem Leibniz-Institut für Meereswissenschaften an der Christian-Albrechts-Universität zu Kiel* (Kiel: Leibniz-Institut für Meereswissenschaften).

Massin, C. (1982). "Food and feeding mechanisms, Holothuroidea," in *Echinoderm Nutrition,* eds M. Jangoux and J. Lawrence (Rotterman: Balkema), 43–55.

Mayor, D. J., Thornton, B., Hay, S., Zuur, A. F., Nicol, G. W., McWilliam, J. M., et al. (2012). Resource quality affects carbon cycling in deep-sea sediments. *ISME J.* 6, 1740–1748. doi: 10.1038/ismej.2012.14

Mengerink, K. J., Van Dover, C. L., Ardron, J., Baker, M., Escobar-Briones, E., Gjerde, K., et al. (2014). A call for deep-ocean stewardship. *Science* 344, 696–698. doi: 10.1126/science.1251458

Middelburg, J. (2014). Stable isotopes dissect aquatic food webs from the top to the bottom. *Biogeosciences* 11, 2357–2371. doi: 10.5194/bg-11-2357-2014

Middelburg, J. J., Barranguet, C., Boschker, H. T., Herman, P. M., Moens, T., and Heip, C. H. (2000). The fate of intertidal microphytobenthos carbon: an *in situ* 13C-labeling study. *Limnol. Oceanogr.* 45, 1224–1234. doi: 10.4319/lo.2000.45.6.1224

Miller, R. J., Smith, C. R., DeMaster, D. J., and Fornes, W. L. (2000). Feeding selectivity and rapid particle processing by deep-sea megafaunal deposit feeders: A 234Th tracer approach. *J. Mar. Res.* 58, 653–673. doi: 10.1357/002224000321511061

Moodley, L., Middelburg, J. J., Boschker, H. T., Duineveld, G. C., Pel, R., Herman, P. M., et al. (2002). Bacteria and Foraminifera: key players in a short term deep-sea benthic response to phytodetritus. *Mar. Ecol. Prog. Ser.* 236, 23–29. doi: 10.3354/meps236023

Petersen, S., Krätschell, A., Augustin, N., Jamieson, J., Hein, J., and Hannington, M. D. (2016). News from the seabed–Geological characteristics and resource potential of deep-sea mineral resources. *Mar. Policy* 70, 175–187. doi: 10.1016/j.marpol.2016.03.012

Purser, A., Marcon, Y., Hoving, H.-J. T., Vecchione, M., Piatkowski, U., Eason, D., et al. (2016). Association of deep-sea incirrate octopods with manganese crusts and nodule fields in the Pacific Ocean. *Curr. Biol.* 26, R1247–R1271. doi: 10.1016/j.cub.2016.10.052

Ramirez-Llodra, E., Tyler, P. A., Baker, M. C., Bergstad, O. A., Clark, M. R., Escobar, E., et al. (2011). Man and the last great wilderness: human impact on the deep sea. *PLoS ONE* 6:e22588. doi: 10.1371/journal.pone.0022588

Roberts, D., Moore, H. M., Berges, J., Patching, J. W., Carton, M. W., and Eardly, D. F. (2001). Sediment distribution, hydrolytic enzyme profiles and bacterial activities in the guts of *Oneirophanta mutabilis*, *Psychropotes longicauda* and *Pseudostichopus villosus*: what do they tell us about digestive strategies of abyssal holothurians? *Prog. Oceanogr.* 50, 443–458. doi: 10.1016/S0079-6611(01)00065-9

Smith, C. R., De Leo, F. C., Bernardino, A. F., Sweetman, A. K., and Arbizu, P. M. (2008). Abyssal food limitation, ecosystem structure and climate change. *Trends Ecol. Evol.* 23, 518–528. doi: 10.1016/j.tree.2008.05.002

Sweetman, A. K., Thurber, A. R., Smith, C. R., Levin, L. A., Mora, C., Wei, C.-L., et al. (2017). Major impacts of climate change on deep-sea benthic ecosystems. *Elem. Sci. Anth.* 5:4. doi: 10.1525/elementa.203

Sweetman, A. K., and Witte, U. (2008). Macrofaunal response to phytodetritus in a bathyal Norwegian fjord. *Deep Sea Res. I* 55, 1503–1514. doi: 10.1016/j.dsr.2008.06.004

Thiel, H., and Schriever, G. (1989). *Cruise Report DISCOL 1, Sonne-Cruise 61*. Hamburg: Institut für Hydrobiologie und Fischereiwissenschaft der Universität Hamburg.

Thiel, H., and Tiefsee-Umweltschutz, F. (2001). Evaluation of the environmental consequences of polymetallic nodule mining based on the results of the TUSCH Research Association. *Deep Sea Res. II* 48, 3433–3452. doi: 10.1016/S0967-0645(01)00051-0

Thurber, A., Sweetman, A. K., Narayanaswamy, B., Jones, D. O., Ingels, J., and Hansman, R. (2014). Ecosystem function and services provided by the deep sea. *Biogeosciences* 11, 3941–3963. doi: 10.5194/bg-11-3941-2014

Van Dover, C. L., Ardron, J. A., Escobar, E., Gianni, M., Gjerde, K. M., Jaeckel, A., et al. (2017). Biodiversity loss from deep-sea mining. *Nat. Geosci.* 10, 464–465. doi: 10.1038/ngeo2983

van Oevelen, D., Soetaert, K., and Heip, C. (2012). Carbon flows in the benthic food web of the Porcupine Abyssal Plain: the (un)importance of labile detritus in supporting microbial and faunal carbon demands. *Limnol. Oceanogr.* 57, 645–664. doi: 10.4319/lo.2012.57.2.0645

Vanreusel, A., Hilario, A., Ribeiro, P. A., Menot, L., and Martinez Arbizu, P. (2016). Threatened by mining, polymetallic noduels are required to preserve abyssal epifauna. *Sci. Rep.* 6:26808. doi: 10.1038/srep26808

Wigham, B. D., Hudson, I. R., Billett, D. S. M., and Wolff, G. A. (2003). Is long-term change in the abyssal Northeast Atlantic driven by qualitative changes in export flux? Evidence from selective feeding in deep-sea holothurians. *Prog. Oceanogr.* 59, 409–441. doi: 10.1016/j.pocean.2003.11.003

Woulds, C., Andersson, J., Cowie, G., Middelburg, J., and Levin, L. (2009). The short-term fate of organic carbon in marine sediments: comparing the Pakistan margin to other regions. *Deep Sea Res. II* 56, 393–402. doi: 10.1016/j.dsr2.2008.10.008

Yool, A., Martin, A. P., Anderson, T. R., Bett, B. J., Jones, D. O., and Ruhl, H. A. (2017). Big in the benthos: future change of seafloor community biomass in a global, body size-resolved model. *Glob. Change Biol.* 23, 3554–3566. doi: 10.1111/gcb.13680

Conflict of Interest Statement: The authors declare that the research was conducted in the absence of any commercial or financial relationships that could be construed as a potential conflict of interest.